View metadata, citation and similar papers at core.ac.uk
brought to you by CORE
provided by Elsevier - Publisher Connector

Cell, Vol. 113, 25–36, April 4, 2003, Copyright ©2003 by Cell Press

bantam Encodes a Developmentally Regulated microRNA that Controls Cell Proliferation and Regulates the Proapoptotic Gene *hid* in *Drosophila*

Julius Brennecke, David R. Hipfner, Alexander Stark, Robert B. Russell, and Stephen M. Cohen*
European Molecular Biology Laboratory
Meyerhofstr 1
69117 Heidelberg
Germany

Summary

Cell proliferation, cell death, and pattern formation are coordinated in animal development. Although many proteins that control cell proliferation and apoptosis have been identified, the means by which these effectors are linked to the patterning machinery remain poorly understood. Here, we report that the *bantam* gene of *Drosophila* encodes a 21 nucleotide microRNA that promotes tissue growth. *bantam* expression is temporally and spatially regulated in response to patterning cues. *bantam* microRNA simultaneously stimulates cell proliferation and prevents apoptosis. We identify the pro-apoptotic gene *hid* as a target for regulation by *bantam* miRNA, providing an explanation for *bantam's* anti-apoptotic activity.

Introduction

Growth of tissues and organs during animal development involves careful coordination of the rates of cell proliferation and cell death (reviewed in Conlon and Raff, 1999). Cell proliferation depends on signals to stimulate cell growth and cell division. In addition, cells compete for intercellular survival signals that are required to prevent them from undergoing apoptosis in response to growth stimuli. How these cellular processes are coordinated with pattern formation during animal development is a challenging question in developmental biology (reviewed in Johnston and Gallant, 2002; Prober and Edgar, 2001). Secreted signaling proteins of the Hedgehog, Wingless/Wnt, and Dpp/BMP families control spatial pattern during animal development (reviewed in Neumann and Cohen, 1997b; Teleman et al., 2001). Evidence has also begun to accumulate implicating these signaling proteins in control of imaginal disc growth during *Drosophila* development. Hedgehog and Dpp signaling have been shown to stimulate cell proliferation in the imaginal discs of *Drosophila* (Duman-Scheel et al., 2002; Martin-Castellanos and Edgar, 2002). Dpp is also thought to provide a survival signal (Moreno et al., 2002). Notch and Wingless signaling are required for tissue growth and cell survival (Baonza and Garcia-Bellido, 1999; Chen and Struhl, 1999; de Celis and Garcia Bellido, 1994; Go et al., 1998; Neumann and Cohen, 1996, 1997a; Thompson et al., 2002), and in some circumstances direct exit from cell proliferation (Johnston and Edgar, 1998; Phillips and Whittle, 1993). At the cellular level, the functions of a number of genes involved in control of cell growth and division have been characterized in the imaginal discs, including components of the Insulin/PI3Kinase pathway, the Myc, Ras and E2F oncogenes, and Cyclin D/CDK4 (reviewed in Johnston and Gallant, 2002). In spite of this considerable progress, how intercellular signals coordinate pattern formation with cell proliferation and cell survival remains poorly understood.

The *bantam* locus of *Drosophila* was identified in a gain-of-function screen for genes that affect tissue growth (Hipfner et al., 2002). In this report, we present evidence that the *bantam* gene encodes a 21 nucleotide microRNA (miRNA). miRNAs are small RNAs, typically of 21–23 nucleotides, that direct posttranscriptional regulation of gene expression (reviewed in Ambros, 2001; Ruvkun, 2001). miRNAs are excised by the Dicer RNase complex from longer precursor RNAs that form imperfect hairpin structures (Bernstein et al., 2001; Hutvagner et al., 2001). Typically only one arm of the hairpin is recovered as a mature product. Processing of miRNAs has much in common with the production of the short interfering RNAs that direct RNA-mediated interference (RNAi).

Two mechanisms for regulation of gene expression by miRNAs have been reported (reviewed in Baulcombe, 2002). Target RNAs containing sequences perfectly complementary to the miRNA are cleaved by ribonucleases in the RISC complex (Hutvagner and Zamore, 2002; Martinez et al., 2002; Zeng et al., 2002), as described recently for transcripts encoding *scarecrow*-like family transcription factors in plants (Llave et al., 2002b). Target RNAs containing sequences imperfectly complementary to the miRNA can be subject to translational control (Olsen and Ambros, 1999; Doench et al., 2003). The *let-7* and *lin4* miRNAs of *C. elegans* act in this manner to repress translation of several mRNAs, which control the transitions between larval stages (Lee et al., 1993; Wightman et al., 1993; Ambros, 2000; Olsen and Ambros, 1999; Reinhart et al., 2000; Slack et al., 2000; Pasquinelli and Ruvkun, 2002). Hundreds of miRNAs have been identified in plants and animals (e.g., Lagos-Quintana et al., 2001, 2002; Lau et al., 2001; Lee and Ambros, 2001; Reinhart et al., 2002; Llave et al., 2002a; Mourelatos et al., 2002). Many of these are conserved between closely related species, and some across phyla (e.g., Pasquinelli et al., 2000). Such numbers suggest that miRNAs have diverse and important regulatory roles in organisms. However, apart from the few exceptions mentioned above, their functions are unknown. Our findings assign a role to the miRNA encoded by the *bantam* gene in control of cell proliferation and apoptosis during *Drosophila* development. Further, they provide a link between the mechanisms that control patterning and tissue growth during animal development.

Results

bantam Encodes a microRNA

The *bantam* locus was identified by several EP element insertions clustered in a region of ~41 kb that lacks

*Correspondence: cohen@embl.de

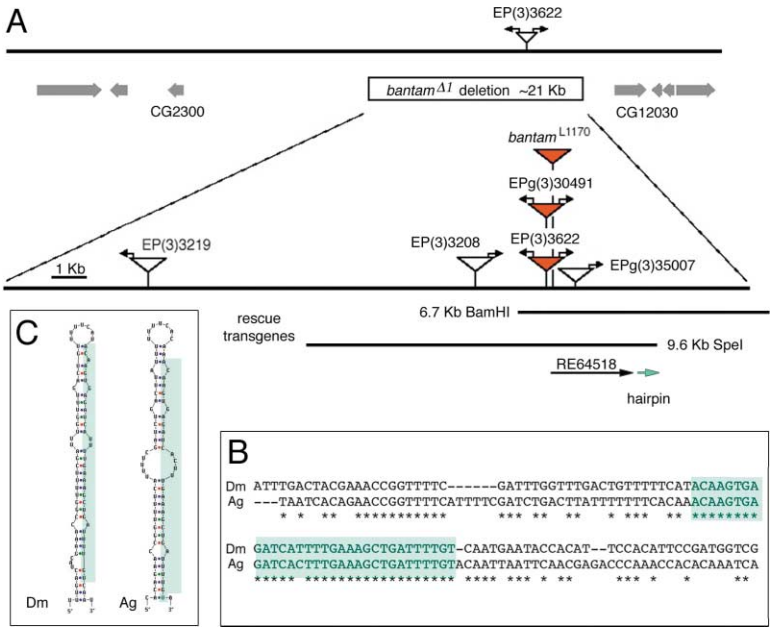

Figure 1. Map of the *bantam* Locus

(A) EP(3)3622 is inserted in a region of 41 kb lacking predicted genes. The extent of the 21 kb *bantam*$^{\Delta 1}$ deletion is indicated by the box and enlarged below. P elements indicated in red are hypomorphic mutant for *bantam*. For EP elements, the arrow indicates the orientation of GAL4-dependent transcription. Rescue transgenes are indicated below. The overlap of the 6.7 kb BamHI and 9.6 kb SpeI fragments defines the minimal essential *bantam* locus. RE64518: arrow indicates the position and size of this cDNA clone (2.2 kb, unspliced). Green arrow: position of a conserved hairpin sequence. The direction of transcription of the predicted hairpin is the same as RE64518. The 3′ end of the EST is 258 bp from the start of the *bantam* hairpin and coincides with a genomic polyA sequence, suggesting that it may represent an artificial priming site for cDNA synthesis in a longer primary transcript. The P element insertional mutants are located upstream from the EST. As these mutants affect the level of miRNA production (Figure 3), we infer that sequences near the 5′ end of the EST are important for production of the primary transcript containing the hairpin. EP(3)35007 is located in RE64518 but does not appear to compromise *bantam* function.

(B) ClustalW alignment of a short sequence conserved between *Anopheles gambiae* (Ag) and *Drosophila melanogaster* (Dm), indicated by the green arrow in (A). Shading indicates the region of highest sequence identity.

(C) Secondary structures for the conserved hairpin sequences. Shading corresponds to (B).

predicted genes (Figure 1A). EP elements are transposable elements designed to allow inducible expression of sequences flanking the insertion site under control of the yeast transcription factor Gal4 (Rorth, 1996). Gal4-dependent expression of the EP elements inserted at the *bantam* locus causes tissue overgrowth due to an increase in cell number. Conversely, flies homozygous for the *bantam*$^{\Delta 1}$ deletion, which removes ~21 kb flanking the insertion site of EP(3)3622 grow poorly and die as early pupae. Flies heterozygous for the *bantam*$^{\Delta 1}$ deletion and three of the P element inserts survived and were morphologically normal but smaller than normal flies. These observations led to the conclusion that the *bantam* locus is involved in growth control during development (Hipfner et al., 2002). In an effort to molecularly define the *bantam* locus, we produced transgenic flies carrying fragments of genomic DNA overlapping the region where P element inserts clustered. Two fragments rescued the growth defects and pupal lethality of flies homozygous for the *bantam*$^{\Delta 1}$ deletion (Figure 1A). The 3.85 kb overlap of these transgenes defines the extent of essential sequences comprising the *bantam* locus. This region contains an EST, RE64518. Expression of RE64518 under Gal4 control failed to reproduce the overgrowth phenotype caused by the EP elements, indicating that RE64518 does not encode *bantam* function (Figure 1A, legend).

The *bantam* region does not have the capacity to encode a protein with significant sequence similarity to proteins in other genomes examined. A BLAST search of the *Anopheles gambiae* genome with the *bantam* region identified a sequence with 30/31 identical residues located 302 nucleotides (nt) downstream from RE64518 (arrow, Figure 1A). Alignment of the two genomic regions containing these sequences with ClustalW identified a block of ~90 residues with considerable similarity (Figure 1B). The *Drosophila* and *Anopheles* sequences were each predicted to fold into stable hairpin structures using mfold (www.bioinfo.rpi.edu/applications/mfold/old/rna/; Figure 1C). The region of highest similarity between these sequences was found on the same arm of the hairpin (shading). These observations suggested that the predicted hairpins might be precursors in the production of a microRNA.

Indeed, a small RNA of ~21 nt was detected by Northern blot analysis of total RNA from third instar larvae, using an end-labeled probe complementary to the conserved 31 nt sequence (Figure 2A, lane 1, arrow). The other arm of the hairpin did not produce a detectable miRNA (not shown). *bantam* miRNA levels were elevated in total RNA from actin-Gal4 > EP(3)3622 larvae (lane 2) and by Gal4-directed expression of the 6.7 kb BamHI genomic rescue fragment (UAS-A; lane 3. Note that UAS-A is in the antisense orientation relative to the vector, see legend, Figure 2C). A larger product was also detected, which may represent the hairpin precursor. To define more precisely the sequences necessary to produce the *bantam* miRNA, we cloned a 584 nt fragment containing the predicted hairpin into the 3′UTR of a heterologous transcript (UAS-C, Figure 2C). Expression of UAS-C under engrailed-Gal4 control also led to overproduction of *bantam* miRNA (Figure 2A, lane 4). *bantam* miRNA was absent from larvae homozygous for the *bantam*$^{\Delta 1}$ deletion (lane 5). Both products were detected in Schneider S2 cells (lane 6). S1 nuclease mapping was used to identify the 5′ and 3′ ends of the miRNA (Figure 2B). The deduced product is the 21 nt miRNA 5′-GUGAGAUCAUUUUGAAAGCUG.

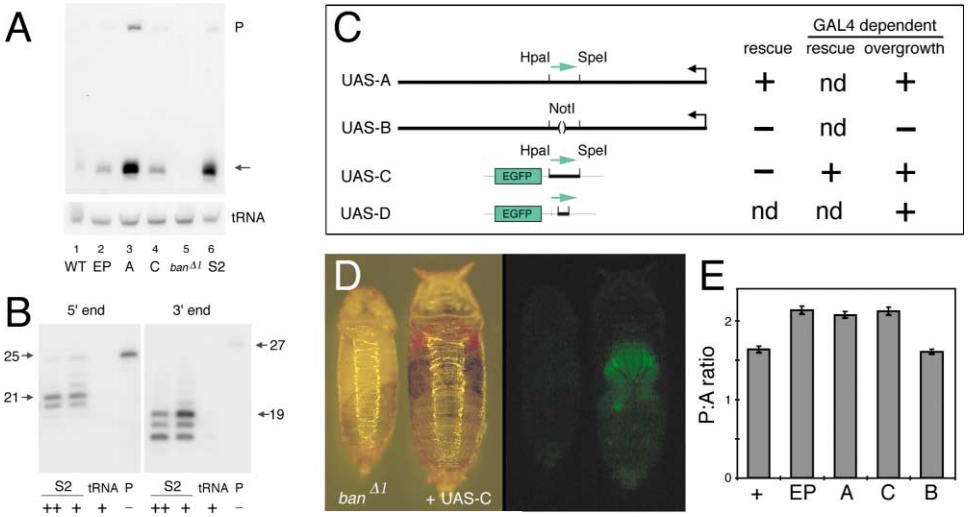

Figure 2. *bantam* Encodes a miRNA

(A) Northern blot comparing *bantam* miRNA levels. Lanes 1–5: third instar larvae. WT: wild-type; EP: Actin-Gal4 > EP(3)3622; A: Actin-Gal4 > UAS-A; C: engrailed-Gal4 > UAS-C. Constructs are depicted in (C). Lane 5: *bantam*$^{\Delta 1}$ mutant larvae. Lane 6: S2 cells. Arrow: 21 nt *bantam* miRNA. P: precursor. The blot was probed with a 31 nt 5′ end-labeled oligonucleotide complementary to the green-shaded side of the stem in Figure 1C.

(B) S1 nuclease-protection mapping of the 5′ and 3′ ends of *bantam* miRNA. Lanes labeled + and ++ denote different amounts of S1 nuclease. Lanes labeled P show end-labeled probes not treated with S1 nuclease. A 21 nt fragment of the 5′ end probe was protected. A19 nt fragment of the 3′ end-labeled probe was protected.

(C) UAS transgenes. The green arrow indicates the predicted hairpin. Rescue assays were performed in the absence of a GAL4 driver. Overgrowth was assayed using engrailed-Gal4. A UAS construct containing the 6.7 kb BamHI fragment transcribed in the sense orientation rescued the mutant in the absence of Gal4, but caused pupal lethality when overexpressed under Gal4 control (not shown). UAS-A is the 6.7 kb BamHI fragment in antisense orientation relative to the pUAST vector. UAS-A contains the endogenous promoter and primary transcript, as it too rescued the mutant in the absence of Gal4. Apparently, Gal4-dependent transcription increases activity of the endogenous promoter on the opposite strand (A). UAS-B is the same as UAS-A, except that it lacks 81 nt containing the predicted hairpin. UAS-C is the 584 nt HpaI-SpeI fragment cloned into the 3′UTR of UAS-EGFP. (This fragment does not overlap with EST RE64518). UAS-D is a 100 nt fragment including the hairpin cloned into the 3′UTR of UAS-EGFP.

(D) Homozygous *bantam*$^{\Delta 1}$ deletion mutant pupae. The pupa at right also expressed UAS-C under armadillo-GAL4 control. Left: bright field image. Right: epifluorescence image showing GFP. Note the restoration of adult structures visible through the pupal case (the eyes are red, wings appear dark).

(E) Quantitation of overgrowth in the wing expressed as the ratio of P:A area. P = the area bounded by vein 4 and the posterior of the wing. A = the area anterior to vein 3, as described in Hipfner et al. (2002). The following transgenes were expressed under engrailed-Gal4 control: EP, EP(3)3622; (A, B, and C) refer to the constructs in (C). +, no UAS transgene.

To verify that the miRNA produced by the predicted hairpin is the functional product of the *bantam* locus, we performed a series of rescue assays and gain of function overgrowth assays. *bantam*$^{\Delta 1}$ homozygous mutant larvae generally lack some or all imaginal discs and show undergrowth of larval tissues including the brain. These animals develop slowly, but survive larval development and die shortly after pupation, lacking evidence of imaginal structures (Figure 2D). As noted above, UAS-A was able to rescue growth of the imaginal discs and allowed the *bantam*$^{\Delta 1}$ homozygous mutant animals to overcome pupal lethality, so that viable adults were produced. Although the construct is in a UAS vector, rescue was independent of GAL4, suggesting that the endogenous regulatory elements needed to produce the *bantam* miRNA are contained within this fragment. However, the surviving flies often had rough eyes, duplicated bristles, and missing halteres, suggesting that some regulatory elements may be missing. When provided with a weak ubiquitous source of GAL4, the 584 nt fragment contained in UAS-C rescued the growth defect in the imaginal discs. Approximately half of the larvae formed morphologically normal pupae that expressed the GFP transgene from which the miRNA is excised (Figure 2D). Many of these animals survived to adulthood. Thus, sequences contained within the 584 nt fragment are sufficient to provide *bantam* function when expressed. The UAS-B transgene contains the same DNA fragment as UAS-A, except that it lacks 81 nt containing the hairpin (Figure 2C). UAS-B was unable to rescue the mutant phenotype, indicating that the deleted residues are essential for *bantam* function. When expressed under engrailed-GAL4 control, constructs UAS-A, UAS-C, and a shorter construct UAS-D containing 100 nt including the hairpin each produced overgrowth of the posterior compartment of the wing and of segments in the larval body (Figure 2E; Supplemental Figure S1 available at http://www.cell.com/cgi/content/full/113/1/25/DC1). UAS-B did not produce any overexpression phenotype. Together these observations assign *bantam* function to the region containing the hairpin and suggest that the 21 nt miRNA is the *bantam* gene product.

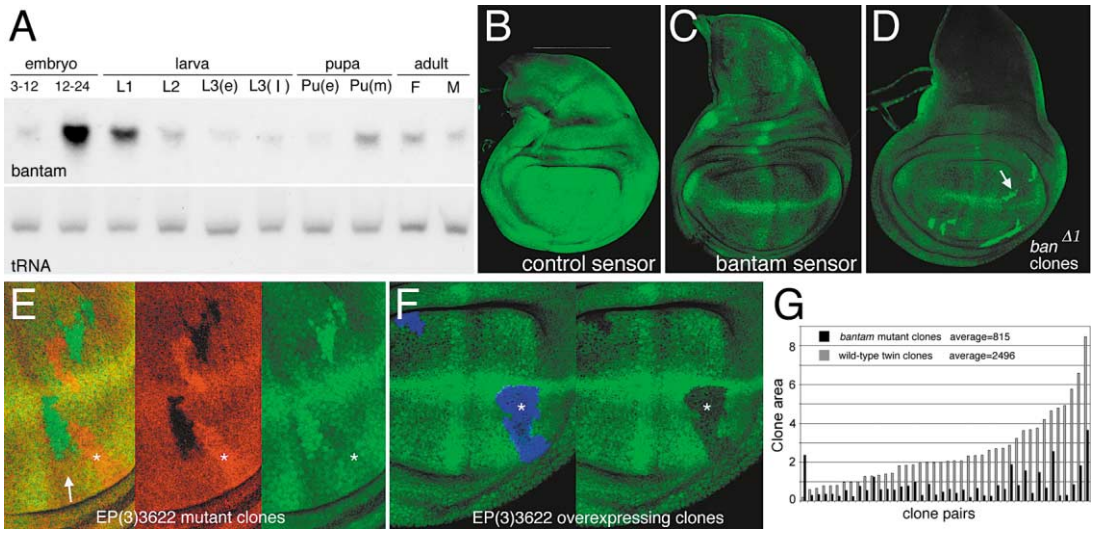

Figure 3. *bantam* miRNA Expression

(A) Northern blot showing *bantam* miRNA at different stages of development. Lanes: 3–12 hr and 12–24 hr old embryos; first, second, early, and late third larval stages; early and mid pupal stages; female and male adults. tRNA, loading control.

(B and C) Wing discs expressing the tubulin-EGFP reporter gene imaged with identical confocal microscope settings.

(B) Control sensor transgene lacking *bantam* target sequences.

(C) *bantam* sensor transgene containing two copies of a 31 nt sequence perfectly complementary to the conserved sequence highlighted in Figure 1C.

(D and E) Wing discs carrying the *bantam* sensor transgene containing clones of cells homozygous for (D) the *bantam*$^{\Delta 1}$ deletion mutant or (E) the *bantam* hypomorphic allele EP(3)3622. Mutant clones showed cell autonomous elevation of *bantam* sensor levels (arrows). Clones were marked by the absence of a lacZ reporter gene (red, not shown in D). (E) Asterisks indicate reduced expression of the sensor in the twin spot clone homozygous wild-type for the *bantam* locus.

(F) Wing disc showing reduced *bantam* sensor levels in a clone of cells overexpressing *bantam* miRNA using EP(3)3622. Larval genotype: HsFlp/Act > CD2 > Gal4; UAS-lacZ; sensor transgene (III)/EP(3)3622. Clones were marked by anti-βgal (blue).

(G) Area measurements of 42 pairs of homozygous *bantam*$^{\Delta 1}$ mutant and wild-type twin clones (scale: thousand pixels). The wild-type and mutant cells are produced in the same cell division, so differences in clone area reflect differences in growth or cell survival after clone induction.

Spatial Control of *bantam* Expression

bantam miRNA was expressed at all developmental stages, though at varying levels (Figure 3A). To ask whether *bantam* expression is spatially regulated during development, we developed an assay based on the ability of miRNAs to inactivate genes by RNAi (Hutvagner and Zamore, 2002; Martinez et al., 2002; Zeng et al., 2002). We prepared a transgene expressing GFP under control of the tubulin promoter and placed two copies of a perfect *bantam* target sequence in the 3′UTR. A comparable construct without the *bantam* target sequences in the 3′UTR was used as a control. Where present, *bantam* miRNA should reduce expression of the transgene containing the target sequences by RNAi, providing an in vivo sensor for *bantam* activity. When expression of the two transgenes was compared using the same settings on the confocal microscope, it was apparent that the control transgene was expressed at much higher levels overall (Figures 3B and 3C). The *bantam* sensor transgene showed a complex pattern of spatial modulation in the third instar wing disc, being higher in cells near the anteroposterior and dorsoventral boundaries and in patches in the dorsal thorax. The control transgene showed limited spatial modulation.

The difference in the overall levels of control and *bantam* sensor transgenes suggested that *bantam* miRNA is expressed broadly in the wing disc, lowering the expression of the specific sensor transgene. Indeed, removing *bantam* miRNA in clones of cells homozygous for the *bantam*$^{\Delta 1}$ deletion increased expression of the *bantam* sensor (Figure 3D). The level of sensor expression in the clones was considerably higher than the maximal endogenous level at the DV boundary, indicating that the miRNA is present throughout the disc, though at varying levels. The P element EP(3)3622 is inserted 2.7 kb from the hairpin and has previously been identified as a hypomorphic allele of *bantam* (Hipfner et al., 2002). Clones of cells homozygous mutant for EP(3)3622 also showed upregulation of the *bantam* sensor (Figure 3E), demonstrating that this insertion reduces *bantam* miRNA levels. In this case, the maximal level of sensor expression was similar to the level at the DV boundary. We noted that the level of sensor expression was lower in the twin spots, which express two copies of the endogenous *bantam* gene than in the surrounding cells, which have one wild-type and one mutant copy of the gene (Figure 3E). This suggested that elevated *bantam* activity would reduce sensor expression. Indeed, clones overexpressing *bantam* reduced sensor levels (Figure 3F). The control sensor was not affected by overexpression of *bantam* (not shown). Taken together, these observations indicate that the sensor is capable of reflecting even subtle increases and decreases in *bantam* miRNA levels in vivo. In all

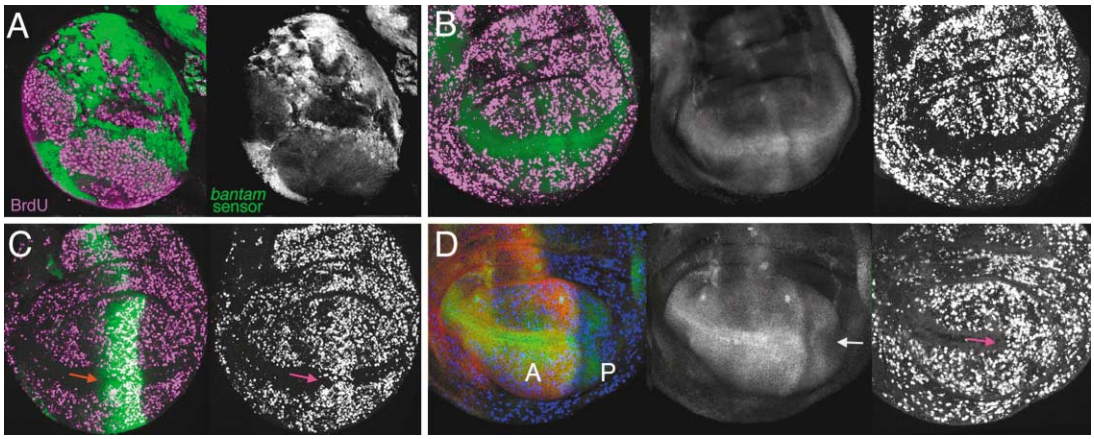

Figure 4. *bantam* Expression and Cell Proliferation

(A) *bantam* sensor levels (green) are low in proliferating cells of the brain hemisphere (labeled by BrdU incorporation, purple), and higher in non proliferating cells.

(B) Wing disc expressing the *bantam* miRNA sensor during late third instar. Sensor expression was elevated in the ZNC. BrdU and sensor images shown separately at right.

(C) Wing disc expressing UAS-C and EGFP under ptc-Gal4 control (green) labeled by BrdU incorporation. Arrow: cells in the ZNC that underwent DNA synthesis due to *bantam* expression.

(D) Wing disc expressing Dfz2-GPI under engrailed-GAL4 control. Anterior cells are labeled red with antibody to fused protein. Sensor expression (green) and BrdU incorporation (blue) are shown separately at right. Sensor levels were lower (white arrow) and ZNC cells incorporated BrdU (red arrow) in the P compartment.

cases, the effects on the sensor were cell autonomous. The sensor transgene method may provide a generally useful tool to visualize miRNA activity in vivo.

bantam Controls Proliferation Cell Autonomously

In light of the observation that *bantam* acts cell autonomously to regulate sensor expression, we asked whether *bantam* acts autonomously to control cell proliferation. FLP-induced mitotic recombination was used to produce clones of cells homozygous for the *bantam*$^{\Delta 1}$ deletion and sister clones that were homozygous wild-type. Each pair of clones derives from a single cell division. Consequently, growth rates can be compared by measuring the areas of individual pairs of mutant and wild-type twin clones after a period of time. Clones were generated at the end of second instar and analyzed late in third instar. Mutant clones were on average 1/3 the size of the wild-type twins (42 pairs, Figure 3G). Although a few relatively large *bantam* mutant clones were observed, mutant clones were typically very small. DAPI labeling did not reveal an observable difference in the size or spacing of nuclei in mutant and wild-type tissue, suggesting that cell size was unaffected by the deletion mutant (not shown; cell size was unchanged in wings of viable hypomorphic mutant combinations; Hipfner et al., 2002). We did not observe an obvious increase in apoptosis in these clones. These observations suggest that *bantam* acts cell autonomously to control cell proliferation.

Developmental Regulation of *bantam* Controls Cell Proliferation

The *bantam* sensor transgene provided a means to compare *bantam* activity and cell proliferation in vivo. Cell proliferation was visualized using BrdU incorporation to label cells undergoing DNA synthesis. We observed a striking correlation between *bantam* activity and cell proliferation in the developing larval brain (Figure 4A). Proliferating cells had a lower level of sensor expression, indicating elevated *bantam* miRNA activity compared to adjacent nonproliferating cells. This correlation was also observed in the wing disc (Figure 4B). Elevated sensor levels coincided with the zone of nonproliferating cells adjacent to the dorsoventral boundary (ZNC; O'Brochta and Bryant, 1985), indicating that *bantam* miRNA levels were reduced in the ZNC.

To ask whether regulation of *bantam* miRNA contributed to the exit of ZNC cells from proliferation, we expressed *bantam* under ptc-Gal4 control. Restoring *bantam* expression was sufficient to direct cells in the nonproliferating zone to enter S phase (arrow, Figure 4C). The ZNC depends on the activity of the secreted signaling protein Wingless and on Notch activity (Phillips and Whittle, 1993; Johnston and Edgar, 1998). Myc expression is downregulated in the ZNC by Wingless signaling. Forced expression of Myc in the ZNC can drive G1-arrested cells into S phase, but does not affect the G2-arrested cells (Johnston et al., 1999; Prober and Edgar, 2002). Although *bantam* can drive both G1/S and G2/M transitions when expressed in the wing disc (Hipfner et al., 2002), *bantam* expression did not affect Myc protein levels in the ZNC (not shown), suggesting that the *myc* transcript is not a target of *bantam* regulation.

The correlation between elevated sensor expression and the ZNC suggested that Wingless might control cell proliferation in the ZNC by reducing *bantam* miRNA levels. To test this, we made use of a dominant-negative form of the Wingless receptor DFz2 to locally reduce

Wingless activity (Cadigan et al., 1998; Zhang and Carthew, 1998). Expression of DFz2-GPI under engrailed-Gal4 control reduced *bantam* sensor levels in the ZNC of the posterior compartment (arrows, Figure 4D), indicating that *bantam* miRNA expression increased when Wingless signaling was impaired. Consequently, cells in the posterior ZNC continued to undergo DNA synthesis and were labeled by BrdU incorporation. Comparable results were obtained by overexpression of the Wingless-pathway inhibitor *naked* (Zeng et al., 2000; not shown). These observations indicate that Wnt signaling contributes to *bantam* miRNA expression to exert developmental control over cell proliferation in the ZNC. We note that the entire posterior compartment is small under these conditions because Wingless is required earlier to promote overall growth of the wing pouch, in addition to its later role in specifying the ZNC. We also noted a second area of reduced *bantam* sensor expression immediately anterior to the AP boundary (e.g., Figure 4D), where Hedgehog signaling has been shown to induce cell proliferation (Duman-Scheel et al., 2002). These observations provide a link between signaling proteins that serve as morphogens to control spatial pattern and *bantam,* a regulator of cell proliferation.

bantam miRNA Is Antiapoptotic

Studies on the Myc and E2F oncogenes in vertebrates have shown that strong proliferative stimuli induce apoptosis (Evan et al., 1994; Dyson, 1998; Harbour and Dean, 2000; Pelengaris et al., 2002). Cell proliferation results only when apoptosis is simultaneously prevented. Overexpression of E2F with its cofactor DP caused apoptosis in the *Drosophila* wing disc, and net cell proliferation resulted only when apoptosis was blocked by coexpression of the caspase inhibitor P35 (Neufeld et al., 1998). In contrast, stimulation of growth by *bantam* overexpression was not associated with an increase in apoptosis (not shown). This raised the possibility that *bantam* might stimulate cell proliferation and simultaneously suppress apoptosis. We therefore asked whether *bantam* could suppress proliferation-induced apoptosis, caused by E2F and DP. Cells expressing E2F and DP under ptc-GAL4 overproliferated, indicated by increased nuclear density in apical optical sections (Figure 5A). In basal optical sections, elevated levels of activated caspase 3 were seen (Figure 5B). Many of these cells dropped out of the epithelial layer and had pyknotic nuclei, indicative of apoptosis. Coexpression of *bantam* enhanced the overproliferation phenotype, indicated by the broader region of high nuclear density (Figure 5C) and reduced the levels of activated caspase (Figure 5D). Fewer cells showed pyknotic nuclei, although many cells did drop out of the epithelial layer, indicating that they were not entirely healthy. Even the modest level of *bantam* overexpression produced by EP(3)3622 was sufficient to suppress apoptosis induced by E2F and DP overexpression.

bantam Regulates *hid* Expression

To identify targets of the *bantam* miRNA, we developed a computational method based on the known *C. elegans* miRNA-target pairs and our general understanding of RNA-RNA interactions (to be described elsewhere). A target search using *bantam* miRNA revealed three independent targets in the 3′UTR of the apoptosis-inducing gene *hid* (Grether et al., 1995). By visual inspection of the 3′UTR of *hid*, we identified two additional sequences complementary to the *bantam* miRNA. All five target sites are highly conserved in the predicted *hid* 3′UTR of *D. pseudoobscura* (Figure 6A). The *bantam* precursor hairpin from *D. pseudoobscura* is identical to that from *D. melanogaster*, except for one base in the terminal loop that is not in the miRNA product. The conservation of these sequences suggests a conserved functional relationship between *bantam* and *hid*.

To assess the function of the predicted *bantam* target sites, we produced a tubulin-EGFP sensor transgene using the 3′UTR of the *hid* mRNA. The resulting GFP pattern was identical to that produced by the *bantam* sensor (Figure 6B, compare with Figure 3C). In addition, the *hid* UTR sensor was downregulated when EP(3)3622 was overexpressed under ptc-Gal4 control (Figure 6C), indicating that the *hid* UTR confers *bantam*-dependent regulation on the transgene. We compared the *hid* UTR sensor with a version from which *bantam* target sites one and four were deleted. The mutated sensor with the three gapped *bantam* sites showed a similar pattern to the complete *hid* UTR sensor, but was downregulated less strongly by endogenous *bantam* (Figure 6D). Overexpressed *bantam* reduced its expression, but the difference in magnitude was less than for the intact *hid* UTR sensor with five sites. These observations indicate that the gapped sites are functional in mediating *bantam* induced repression, but show that five sites mediate stronger repression than three sites. Cooperativity among multiple sites has recently been reported for siRNA-mediated translational repression (Doench et al., 2003).

bantam Blocks *hid*-Induced Apoptosis

Having shown that *bantam* can block expression of a transgene containing the *hid* 3′UTR, we asked whether *bantam* regulates the endogenous *hid* gene. *hid* was expressed from EP(3)30060 under ptc-Gal4 control, either alone or together with EP(3)3622. Hid protein levels were reduced by coexpression with *bantam* (Figures 7A and 7D), but *hid* transcript levels were comparable (Figures 7B and 7E). This indicates that Hid protein expression is repressed by *bantam,* most likely by blocking translation of the *hid* mRNA. We next examined the ability of *bantam* to suppress the apoptosis-inducing effects of *hid*. *hid* expression induced apoptosis, visualized by caspase 3 activation (Figure 7C). This was suppressed by coexpression of *bantam* (Figure 7F). These observations show that *bantam* effectively suppresses *hid*-induced apoptosis. The ability of *bantam* to suppress proliferation-induced apoptosis may reflect its ability to block Hid expression, though we do not exclude the possibility of other indirect effects.

Induction of cell death in postmitotic cells of the eye imaginal disc by GMR-hid, GMR-hid(Ala5) and GMR-reaper transgenes leads to a small, rough eye phenotype (Figures 8C, 8F, and 8I; Bergmann et al., 1998; Kurada and White, 1998). Eye size was largely restored by coexpression of *bantam* using GMR-Gal4 to direct expression of EP(3)3622, though suppression of the GMR-hid

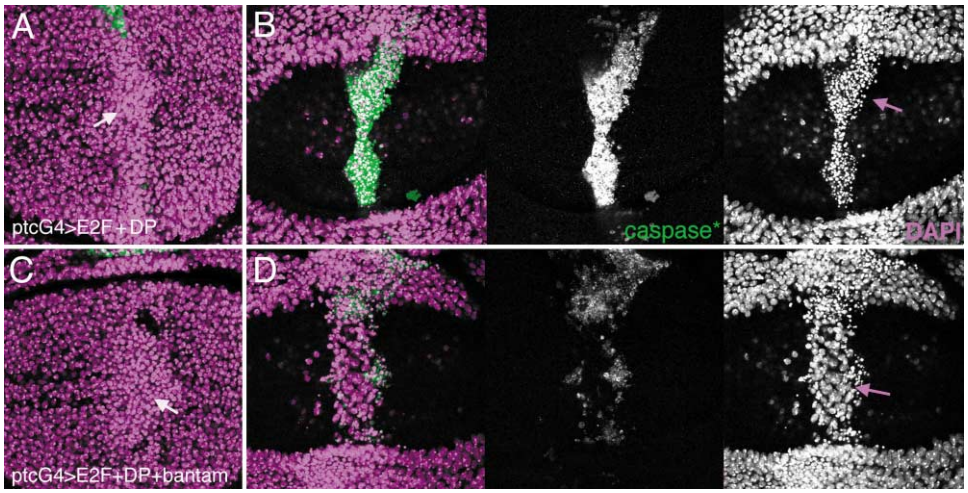

Figure 5. *bantam* Inhibits Proliferation-Induced Apoptosis

Wing discs labeled with antibody to activated caspase (green) to visualize apoptotic cells. DAPI-labeled nuclei (purple). All images were taken with identical settings on the confocal microscope to permit comparison of the intensity of activated caspase.

(A and C) Single apical optical sections.

(B and D) Projections of several optical sections in the basal region of the discs.

(A and B) ptc-GAL4 directed expression of E2F and DP.

(A) Note the increased density of nuclei in the apical section (white arrow).

(B) Dying cells are typically extruded basally. Caspase activation was high in these cells and nuclei were pyknotic (purple arrow).

(C and D) ptc-GAL4 directed expression of E2F and DP with EP(3)3622.

(C) Nuclear density was increased in a broader region than in the disc expressing E2F and DP alone (white arrow), suggesting that fewer cells dropped out of the epithelium.

(D) Caspase activation was reduced and nuclei were mostly not pyknotic (purple arrow).

and GMR-hid(Ala5) phenotypes was much better (Figures 8B, 8E, and 8H). Ommatidial structure was largely restored in the GMR-hid eyes, but not in the GMR-reaper eyes, suggesting a more specific suppression of *hid* activity. Hid(Ala5) has the 5 consensus ERK phosphorylation sites mutated to alanine and cannot be suppressed by activation of the ERK MAPK pathway (Bergmann et al., 1998). The observation that *bantam* coexpression blocks the activity of Hid(Ala5) excludes an indirect effect mediated by regulation of the MAPK pathway. To explore the question of specificity further, we compared the effects of removing one copy of the endogenous *bantam* gene in these three backgrounds. This had a minor effect on the severity of the GMR-reaper, but clearly enhanced the severity of the GMR-hid and GMR-hid(Ala5) phenotypes (Figures 8D, 8G, and 8J). This suggests that endogenous expression of the *bantam* gene in the developing eye imaginal disc contributes to controlling the level of *hid*-induced apoptosis, which is normally involved in reducing cell number in the pupal eye disc (Bergmann et al., 1998; Kurada and White, 1998; Yu et al., 2002).

Discussion

Control of Tissue Growth by a microRNA

In this report, we present evidence that the *bantam* gene of *Drosophila* encodes a miRNA that controls cell proliferation and apoptosis. *bantam*-induced tissue growth results from an increase in cell number due to an increase in the rate of cell proliferation, not from an increase in cell size (Hipfner et al., 2002). The antiapoptotic effects of *bantam* are not sufficient to explain its effects on tissue growth. Expression of the caspase inhibitor P35 effectively blocks apoptosis in vivo but does not cause net tissue growth.

bantam's effects are distinguishable from those of Ras, Myc, and the insulin/PI3K pathway, which primarily affect cellular growth (Johnston et al., 1999; Prober and Edgar, 2000, 2002; reviewed in Stocker and Hafen, 2000). The effects of *bantam* most closely resemble those caused by altered levels of *cyclinD/CDK4* activity (Datar et al., 2000; Meyer et al., 2000). Like *cyclinD/CDK4*, *bantam* controls cellular growth and cell cycle progression in a coordinated manner.

To understand how *bantam* miRNA promotes cell proliferation and prevents cell death, it will be necessary to identify the genes that it regulates. Using a computational method for predicting possible target genes of miRNAs, we identified the pro-apoptotic gene *hid* as a direct target for regulation by *bantam* miRNA, suggesting one mechanism by which *bantam* contributes to controlling cell death. *bantam* target sequences were not found in any of the following genes: *ras*, *myc*, *dE2F*, *dDP*, *cyclin D*, *CDK4*, *cyclin E*, *string*, or in components of the insulin/PI(3) kinase pathway. If we assume that *bantam* acts as a negative regulator of target genes (as for *hid*), its targets might be negative regulators of cell growth or cell proliferation. We also failed to find *bantam* target sites in the following genes: *PTEN*, *TSC1*, *TSC2*, *salvador*, *warts/lats*, *merlin*, *expanded*, *lethal giant larvae*, *discs large*, and *discs overgrown*. It seems likely

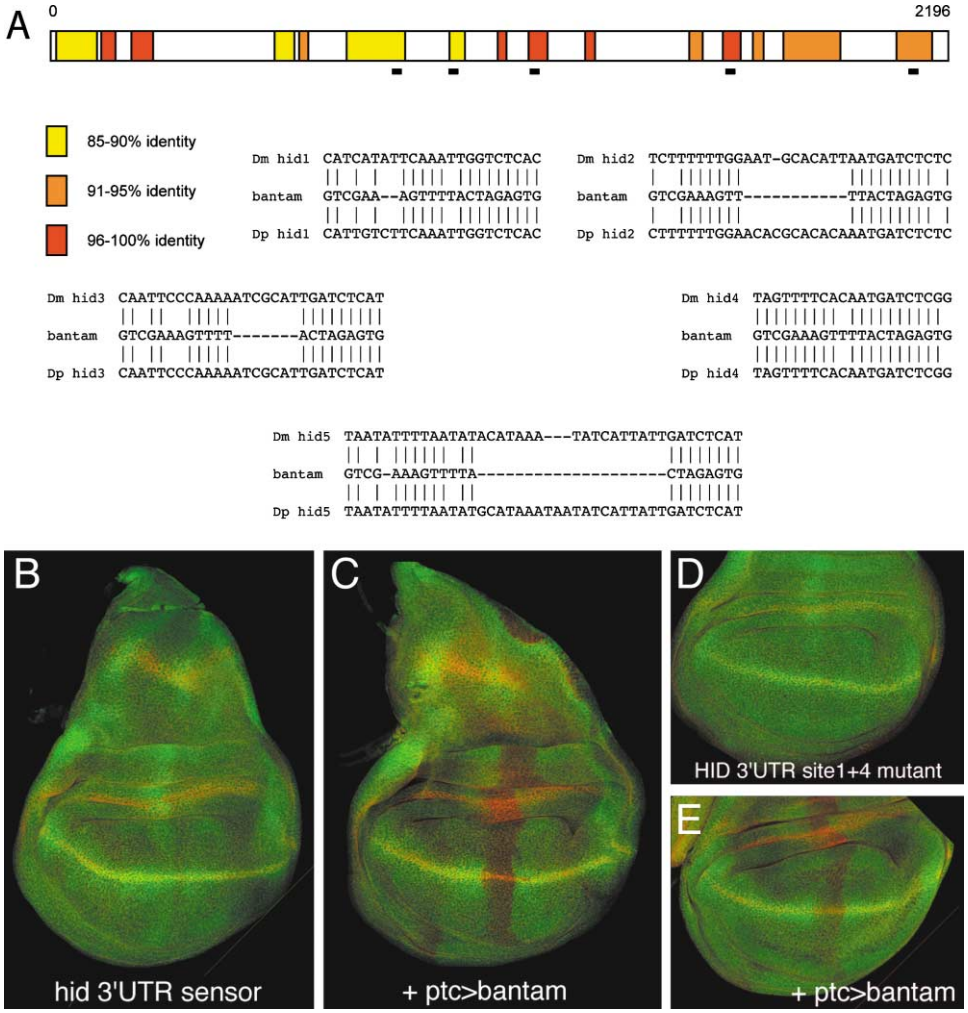

Figure 6. *bantam* Regulates the *hid* 3′UTR

(A) Schematic representation of the 3′UTR of *hid* from *D. melanogaster*. Blocks highly conserved in *D. pseudoobscura* are indicated by color. Alignment of *bantam* miRNA with the predicted target sites from the *hid* UTRs are shown below.

(B) Wing disc showing expression of the Tubulin–EGFP transgene with the *hid* 3′UTR (green). Wg protein (red) is shown to visualize the DV boundary.

(C) As in (B) with ptc-Gal4 directing expression of EP(3)3622.

(D) Wing disc showing expression of the *hid* 3′UTR sensor with *bantam* sites 1 and 4 deleted.

(E) As in (D) with ptc-Gal4 directing expression of EP(3)3622.

that *bantam* may regulate an as yet unidentified negative regulator of cell proliferation. In depth analysis of additional predicted targets will be required to determine how *bantam* controls cell proliferation.

bantam Blocks *hid*-Induced Apoptosis

The three proapoptotic genes *hid*, *reaper*, and *grim* downregulate levels of the IAP proteins in *Drosophila*, thereby preventing caspase activation (Yoo et al., 2002). Unlike *reaper* and *grim*, whose activity appears to be regulated primarily at the transcriptional level, *hid* mRNA is also detected in cells that do not undergo apoptosis (Grether et al., 1995). Evidence has been presented for transcriptional regulation of *hid* (Kurada and White, 1998) and for posttranslational regulation of Hid activity by the MAPK signaling pathway (Bergmann et al., 1998). By showing that *bantam* blocks the activity of Hid(Ala5), which is insensitive to MAPK regulation, we exclude an indirect effect of *bantam* mediated by regulation of the MAPK pathway. We have also shown that the *hid* 3′UTR confers *bantam*-mediated regulation on a heterologous reporter. These findings provide evidence that *hid* is subject to translational regulation in vivo by the *bantam* miRNA.

hid is known to play an important role in regulating apoptosis in eye development (Bergmann et al., 1998; Kurada and White, 1998; Yu et al., 2002). We found that removing one copy of the endogenous *bantam* gene enhanced the severity of the Hid-induced apoptosis phenotype in the eye, whereas the severity of the *reaper*-induced apoptosis phenotype was affected much less

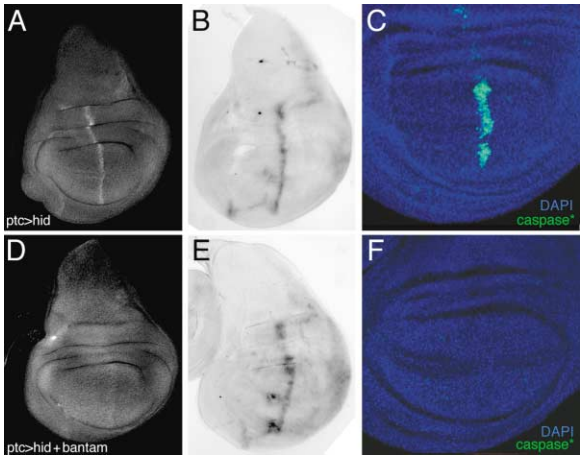

Figure 7. *bantam* Regulates Hid Expression

(A–C) ptc-GAL4 directed expression of *hid* using EP(3)30060 in wing discs.

(D–F) as in (A–C) plus *bantam* expressed by EP(3)3622.

(A and D) Discs labeled with antibody to Hid protein.

(B and E) In situ hybridization with anti-sense RNA probes to detect *hid* mRNA.

(C and F) Discs labeled with antibody to activated caspase 3 (green). DAPI-labeled nuclei (blue). (C and F) are projections of several optical sections.

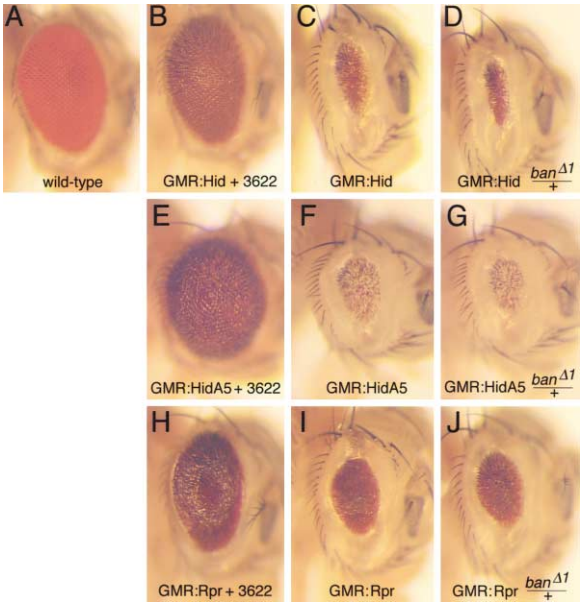

Figure 8. *bantam* Levels Regulate *hid* Activity in Eye Development

(A) Wild-type head showing normal eye size and arrangement of ommatidia.

(B–D) Flies expressing *hid* in postmitotic cells under GMR control.

(E–G) Flies expressing hid^{Ala5} under GMR control.

(H–J) Flies expressing *reaper* under GMR control.

strongly. Similarly, overexpression of *bantam* suppressed both the GMR-hid and GMR-reaper phenotypes, but had a stronger effect on *hid*. Kurada and White (1998) have shown that the severity of the GMR-reaper phenotype is sensitive to the levels of *hid* activity. By overexpressing *bantam*, we have reduced Hid levels, providing an explanation for the observed suppression of the GMR-reaper phenotype. Similarly, by removing one copy of *bantam* we would expect to increase endogenous *hid* activity in the eye. By altering the level of Hid, *bantam* can indirectly alter the threshold for *reaper*-induced apoptosis. This provides an explanation for the slight increase in severity of the GMR-reaper phenotype that we observed. We note that there are no *bantam* target sites in the *reaper* gene, suggesting that *bantam's* effect on the GMR-reaper phenotype must be indirect. Finally, we did not observe an increase in apoptosis in *bantam* mutant clones in the wing disc. To our knowledge, endogenous *hid* has not been implicated in developmental control of cell death in the wing.

Developmental Regulation of *bantam*

The secreted signaling proteins that control spatial pattern during *Drosophila* development also control tissue growth. Hedgehog promotes cell growth and proliferation in the eye and wing discs by inducing cyclin D and cyclin E expression (Duman-Scheel et al., 2002). The Dpp morphogen gradient has been implicated in control of proliferation and appears to provide cell survival cues as well (Martin-Castellanos and Edgar, 2002; Moreno et al., 2002). Wingless appears to act as both a positive and negative regulator of growth in a context-dependent manner in the wing disc (Johnston and Edgar, 1998; Neumann and Cohen, 1996, 1997a). We have presented evidence here that blocking Wnt signaling by overexpression of a dominant-negative form of the Fz2 receptor protein restores cell proliferation in the ZNC, at least in part by regulating *bantam* miRNA expression. It will be of interest to learn whether *bantam* homologs play a comparable role as regulators of cell proliferation during vertebrate embryogenesis. BLAST searches did not find sequences identical to the *bantam* miRNA in the mouse or human genomes, however the possibility exists that a functionally homologous miRNA may differ slightly in nucleotide sequence. The putative *Anopheles* homolog has a single nucleotide alteration. In addition, three cloned *C. elegans* miRNAs, mir80, mir81, and miR82, are similar to *bantam* (Lau et al., 2001; Lee and Ambros, 2001; V. Ambros, personal communication). It remains to be determined if they have a similar function.

Is *bantam* an Oncogene?

The possibility that misexpression or misregulation of *bantam* homologs might be responsible for diseases of cell proliferation is intriguing. *bantam* can suppress apoptosis while stimulating cell proliferation in *Drosophila*. In *Drosophila*, cyclinD/CDK4 overexpression causes a proliferation phenotype similar to *bantam* and their human homologs are oncogenes (reviewed by Ortega et al., 2002). Oncogenes such as Myc and E2F promote apoptosis as well as cell proliferation. Tumor formation requires additional anti-apoptotic inputs (e.g., Pelengaris et al., 2002). *bantam* is able to do both and so its putative vertebrate homologs may be oncogenes. In this context, it is noteworthy that Argonaute family genes, which encode components of the cellular machinery needed to produce miRNAs, have been implicated in

numerous biological processes including tumorigenesis (reviewed by Carmell et al., 2002).

miRNA Genetics

miRNAs are short noncoding sequences and so present small targets for chemical mutagenesis. Identification of *bantam* depended on a gain-of-function genetic strategy making use of EP elements to overexpress genes tagged by P element insertion (Rorth, 1996). Several other miRNAs are located next to EP elements in the *Drosophila* genome, opening the possibility for analysis of their functions in vivo.

Experimental Procedures

Strains

Armadillo-Gal4 (II), engrailed-Gal4, actin-Gal4, GMR-Gal4, GMR:Hid, GMR:Rpr, and ptc-Gal4 are described in flybase (http://fly.bio.indiana.edu/gal4.htm). GMR-hid(Ala5) is described in Bergmann et al. (1998). UAS-naked is described in Zeng et al. (2000). UAS-Dfz2GPI is described in Cadigan et al. (1998). UAS-E2F and UAS-DP are described in Neufeld et al. (1998). EP(3)30060 directs expression of *hid* and was identified by Mata et al. (2000). EP(3)3622 is described in Hipfner et al. (2002).

Transgenes

Genomic Rescue Constructs

9.6 kb SpeI and 6.7 kb BamHI fragments of BAC AC011907 were cloned into pUAST digested with XbaI or BglII (sequence coordinates: BamHI 153603–160352; SpeI 147839–157456). The ability of the transgenes to rescue was assayed in homozygous *bantam*$^{\Delta 1}$ deletion mutant flies lacking a GAL4 driver.

Hairpin Deletion Rescue Construct

Residues 14192–14689 and 14770–15097 of AE003469.3 were PCR amplified with a NotI site added following residue 14689 and preceding 14770. Ligation at the NotI site deleted 81 nt containing the hairpin. This fragment was inserted to replace the HpaI-SpeI fragment in pUAST-BamHI.

Heterologous Hairpin Expression Construct

A 584 nt HpaI-SpeI fragment was cloned into the 3′UTR of UAS-EGFP digested with NotI (end repaired) and XbaI.

bantam *Sensor*

Two copies of the 31 nt conserved sequence in the hairpin were cloned downstream of Tub-EGFP into the 3′UTR derived from the 3′ end of the P element in CaSpeR4.

hid-UTR Sensor

The *hid* 3′UTR was amplified from genomic DNA with the following primers 5′-GTcctaggAAGCGCAGGAGACGTGTAATCG and 5′-GTctcgagGCGCTTTTATTTCATTTACACATAC. The UTR was cloned into the control sensor plasmid as an AvrII-XhoI fragment. To prepare the *hid* 3′UTR with *bantam* sites one and four deleted the following primer pairs were used: for site one, 5′-GTggatccTATGATGATGAACAAACAATGAC and 5′-GTggatccAATATAATAGTTTTAAGCTCCACG and for site four, 5′-GTgcggccgcACTAATTAGCAATAAGCAGGGG and 5′-GTgcggccgcTAAAGTTTTGTGGCCTTGCGCC. At least two independent transgenic strains were assayed for each construct.

bantam Clonal Analysis

Mitotic recombination clones were induced 48 ± 1.5 hr after egg laying (AEL) in staged larvae by heat shock at 37–38°C for 60 min. Larval genotypes: *HS-FLP1*; *armLacZ FRT80B/bantam*$^{\Delta 1}$ *FRT80B* (or *armLacZ FRT80B*/EP(3)3622 FRT80B). Both genotypes were examined with and without the *bantam* sensor on chromosome 2. Discs were dissected at 110 ± 1.5 hr AEL, fixed in 4% formaldehyde, and stained with anti-β-galactosidase antibody to mark the clones, with anti-GFP to visualize sensor expression and with DAPI to mark the nuclei. Clones were analyzed by confocal microscopy. Clone areas were measured using Adobe Photoshop.

Northern Blots

Total RNA was resolved on 15% denaturing acrylamide gels and probed with 5′ end-labeled oligonucleotides as indicated in the text. A tRNA probe was used as a loading control (Lagos-Quintana et al., 2001).

S1 nuclease mapping was performed as described by Hahn (http://www.fhcrc.org/labs/hahn/methods/mol_bio_meth/s1_oligo_probe.html). For 5′ end mapping, the 25-mer 5′-CAGCTTTCAAAATCATCTCACTTGT was 5′ end labeled with polynucleotide kinase. For 3′ end mapping, the 26-mer 5′-GCCAAAATCAGCTTTCAAAATGATCT was annealed to a second oligo 5′-GTGAGATCATTTTGGAAAGCTGA and extended by addition of dCTP with the Klenow fragment of DNA polymerase. Labeled primers were annealed with total RNA from S2 cells at 48°C, digested with S1 nuclease at 20°C, and resolved on 15% denaturing acrylamide gels.

Antibodies

Antibodies include: rabbit anti-Hid (Yoo et al., 2002), mouse anti-Myc (Prober and Edgar, 2000), rabbit anti-GFP (Torrey Pines Laboratories), mouse anti-BrdU (PharMingen), and rabbit antibody to cleaved human caspase-3 (Cell Signaling Technology). An antiserum raised against the same epitope reacts specifically with the cleaved form of the *Drosophila* caspase Drice and labels apoptotic cells (Yu et al., 2002).

Genome sequence data for *D. pseudoobscura* is available at (http://hgsc.bcm.tmc.edu/projects/drosophila/).

Acknowledgments

We thank Ann-Mari Voie and Lidia Pérez for technical assistance. We thank the Tuschl lab for detailed protocols for miRNA Northerns; Bruce Hay for anti-Hid; Bruce Edgar for anti-Myc; Hermann Steller for *hid* cDNA; and Andreas Bergmann for GMR-hid(Ala5) flies.

Received: November 14, 2002
Revised: March 4, 2003
Accepted: March 7, 2003
Published: April 3, 2003

References

Ambros, V. (2000). Control of developmental timing in *Caenorhabditis elegans*. Curr. Opin. Genet. Dev. *10*, 428–433.

Ambros, V. (2001). microRNAs: tiny regulators with great potential. Cell *107*, 823–826.

Baonza, A., and Garcia-Bellido, A. (1999). Notch signaling directly controls cell proliferation in the *Drosophila* wing disc. Proc. Natl. Acad. Sci. USA *97*, 2609–2614.

Baulcombe, D. (2002). DNA events. An RNA microcosm. Science *297*, 2002–2003.

Bergmann, A., Agapite, J., McCall, K., and Steller, H. (1998). The *Drosophila* gene hid is a direct molecular target of Ras-dependent survival signaling. Cell *95*, 331–341.

Bernstein, E., Caudy, A.A., Hammond, S.M., and Hannon, G.J. (2001). Role for a bidentate ribonuclease in the initiation step of RNA interference. Nature *409*, 363–366.

Cadigan, K.M., Fish, M.P., Rulifson, E.J., and Nusse, R. (1998). Wingless repression of *Drosophila* frizzled 2 expression shapes the wingless morphogen gradient in the wing. Cell *93*, 767–777.

Carmell, M.A., Xuan, Z., Zhang, M.Q., and Hannon, G.J. (2002). The Argonaute family: tentacles that reach into RNAi, developmental control, stem cell maintenance, and tumorigenesis. Genes Dev. *16*, 2733–2742.

Chen, C.M., and Struhl, G. (1999). Wingless transduction by the frizzled and frizzled2 proteins of Drosophila. Development *126*, 5441–5452.

Conlon, I., and Raff, M. (1999). Size control in animal development. Cell *96*, 235–244.

Datar, S.A., Jacobs, H.W., de La Cruz, A.F., Lehner, C.F., and Edgar, B.A. (2000). The *Drosophila* cyclin D-cdk4 complex promotes cellular growth. EMBO J. *19*, 4543–4554.

de Celis, J.F., and Garcia Bellido, A. (1994). Roles of the *notch* gene in *Drosophila* wing morphogenesis. Mech. Dev. *46*, 109–122.

Doench, J.G., Petersen, C.P., and Sharp, P.A. (2003). siRNAs can function as miRNAs. Genes Dev. *17*, 438–442.

Duman-Scheel, M., Weng, L., Xin, S., and Du, W. (2002). Hedgehog regulates cell growth and proliferation by inducing Cyclin D and Cyclin E. Nature *417*, 299–304.

Dyson, N. (1998). The regulation of E2F by pRB-family proteins. Genes Dev. *12*, 2245–2262.

Evan, G., Harrington, E., Fanidi, A., Land, H., Amati, B., and Bennett, M. (1994). Integrated control of cell proliferation and cell death by the c-myc oncogene. Philos. Trans. R. Soc. Lond. B Biol. Sci. *345*, 269–275.

Go, M.J., Eastman, D.S., and Artavanis-Tsakonas, S. (1998). Cell proliferation control by notch signaling in *Drosophila* development. Development *125*, 2031–2040.

Grether, M.E., Abrams, J.M., Agapite, J., White, K., and Steller, H. (1995). The head involution defective gene of *Drosophila melanogaster* functions in programmed cell death. Genes Dev. *9*, 1694–1708.

Harbour, J.W., and Dean, D.C. (2000). Rb function in cell-cycle regulation and apoptosis. Nat. Cell Biol. *2*, E65–E67.

Hipfner, D.R., Weigmann, K., and Cohen, S.M. (2002). The bantam gene regulates *Drosophila* growth. Genetics *161*, 1527–1537.

Hutvagner, G., and Zamore, P.D. (2002). A microRNA in a multiple-turnover RNAi enzyme complex. Science *297*, 2056–2060.

Hutvagner, G., McLachlan, J., Pasquinelli, A.E., Balint, E., Tuschl, T., and Zamore, P.D. (2001). A cellular function for the RNA-interference enzyme dicer in the maturation of the let-7 small temporal RNA. Science *293*, 834–838.

Johnston, L.A., and Edgar, B.A. (1998). Wingless and notch regulate cell-cycle arrest in the developing *Drosophila* wing. Nature *394*, 82–84.

Johnston, L.A., and Gallant, P. (2002). Control of growth and organ size in *Drosophila*. Bioessays *24*, 54–64.

Johnston, L.A., Prober, D.A., Edgar, B.A., Eisenman, R.N., and Gallant, P. (1999). *Drosophila* myc regulates cellular growth during development. Cell *98*, 779–790.

Kurada, P., and White, K. (1998). Ras promotes cell survival in *Drosophila* by downregulating hid expression. Cell *95*, 319–329.

Lagos-Quintana, M., Rauhut, R., Lendeckel, W., and Tuschl, T. (2001). Identification of novel genes coding for small expressed RNAs. Science *294*, 853–858.

Lagos-Quintana, M., Rauhut, R., Yalcin, A., Meyer, J., Lendeckel, W., and Tuschl, T. (2002). Identification of tissue-specific MicroRNAs from mouse. Curr. Biol. *12*, 735–739.

Lau, N.C., Lim, L.P., Weinstein, E.G., and Bartel, D.P. (2001). An abundant class of tiny RNAs with probable regulatory roles in *Caenorhabditis elegans*. Science *294*, 858–862.

Lee, R.C., and Ambros, V. (2001). An extensive class of small RNAs in *Caenorhabditis elegans*. Science *294*, 862–864.

Lee, R.C., Feinbaum, R.L., and Ambros, V. (1993). The *C. elegans* heterochronic gene lin-4 encodes small RNAs with antisense complementarity to lin-14. Cell *75*, 843–854.

Llave, C., Kasschau, K.D., Rector, M.A., and Carrington, J.C. (2002a). Endogenous and silencing-associated small RNAs in plants. Plant Cell *14*, 1605–1619.

Llave, C., Xie, Z., Kasschau, K.D., and Carrington, J.C. (2002b). Cleavage of scarecrow-like mRNA targets directed by a class of *Arabidopsis* miRNA. Science *297*, 2053–2056.

Martin-Castellanos, C., and Edgar, B.A. (2002). A characterization of the effects of Dpp signaling on cell growth and proliferation in the *Drosophila* wing. Development *129*, 1003–1013.

Martinez, J., Patkaniowska, A., Urlaub, H., Luhrmann, R., and Tuschl, T. (2002). Single-stranded antisense siRNAs guide target RNA cleavage in RNAi. Cell *110*, 563-574.

Mata, J., Curado, S., Ephrussi, A., and Rorth, P. (2000). Tribbles coordinates mitosis and morphogenesis in *Drosophila* by regulating string/CDC25 proteolysis. Cell *101*, 511–522.

Meyer, C.A., Jacobs, H.W., Datar, S.A., Du, W., Edgar, B.A., and Lehner, C.F. (2000). *Drosophila* cdk4 is required for normal growth and is dispensable for cell cycle progression. EMBO J. *19*, 4533–4542.

Moreno, E., Basler, K., and Morata, G. (2002). Cells compete for decapentaplegic survival factor to prevent apoptosis in *Drosophila* wing development. Nature *416*, 755–759.

Mourelatos, Z., Dostie, J., Paushkin, S., Sharma, A., Charroux, B., Abel, L., Rappsilber, J., Mann, M., and Dreyfuss, G. (2002). miRNPs: a novel class of ribonucleoproteins containing numerous microRNAs. Genes Dev. *16*, 720–728.

Neufeld, T.P., de la Cruz, A.F., Johnston, L.A., and Edgar, B.A. (1998). Coordination of growth and cell division in the *Drosophila* wing. Cell *93*, 1183–1193.

Neumann, C.J., and Cohen, S.M. (1996). Distinct mitogenic and cell fate specification functions of wingless in different regions of the wing. Development *122*, 1781–1789.

Neumann, C.J., and Cohen, S.M. (1997a). Long-range action of wingless organizes the dorsal-ventral axis of the *Drosophila* wing. Development *124*, 871–880.

Neumann, C.J., and Cohen, S.M. (1997b). Morphogens and pattern formation. Bioessays *19*, 721–729.

O'Brochta, D.A., and Bryant, P.J. (1985). A zone of non-proliferating cells at a lineage restriction boundary in *Drosophila*. Nature *313*, 138–141.

Olsen, P.H., and Ambros, V. (1999). The lin-4 regulatory RNA controls developmental timing in *Caenorhabditis elegans* by blocking LIN-14 protein synthesis after the initiation of translation. Dev. Biol. *216*, 671–680.

Ortega, S., Malumbres, M., and Barbacid, M. (2002). Cyclin D-dependent kinases, INK4 inhibitors and cancer. Biochim. Biophys. Acta *1602*, 73–87.

Pasquinelli, A.E., Reinhart, B.J., Slack, F., Martindale, M.Q., Kuroda, M.I., Maller, B., Hayward, D.C., Ball, E.E., Degnan, B., Muller, P., et al. (2000). Conservation of the sequence and temporal expression of let-7 heterochronic regulatory RNA. Nature *408*, 86–89.

Pasquinelli, A.E., and Ruvkun, G. (2002). Control and developmental timing by microRNAs and their targets. Annu. Rev. Cell Dev. Biol. *18*, 495–513.

Pelengaris, S., Khan, M., and Evan, G.I. (2002). Suppression of Myc-induced apoptosis in beta cells exposes multiple oncogenic properties of Myc and triggers carcinogenic progression. Cell *109*, 321–334.

Phillips, R., and Whittle, J.R.S. (1993). *wingless* expression mediates determination of peripheral nervous system elements in late stages of *Drosophila* wing disc development. Development *118*, 427–438.

Prober, D.A., and Edgar, B.A. (2000). Ras1 promotes cellular growth in the *Drosophila* wing. Cell *100*, 435–446.

Prober, D.A., and Edgar, B.A. (2001). Growth regulation by oncogenes–new insights from model organisms. Curr. Opin. Genet. Dev. *11*, 19–26.

Prober, D.A., and Edgar, B.A. (2002). Interactions between Ras1, dMyc, and dPI3K signaling in the developing *Drosophila* wing. Genes Dev. *16*, 2286–2299.

Reinhart, B.J., Slack, F.J., Basson, M., Pasquinelli, A.E., Bettinger, J.C., Rougvie, A.E., Horvitz, H.R., and Ruvkun, G. (2000). The 21-nucleotide let-7 RNA regulates developmental timing in *Caenorhabditis elegans*. Nature *403*, 901–906.

Reinhart, B.J., Weinstein, E.G., Rhoades, M.W., Bartel, B., and Bartel, D.P. (2002). MicroRNAs in plants. Genes Dev. *16*, 1616–1626.

Rorth, P. (1996). A modular misexpression screen in *Drosophila* detecting tissue specific phenotypes. Proc. Natl. Acad. Sci. USA *93*, 12418–12422.

Ruvkun, G. (2001). Molecular biology. Glimpses of a tiny RNA world. Science *294*, 797–799.

Slack, F.J., Basson, M., Liu, Z., Ambros, V., Horvitz, H.R., and Ruvkun, G. (2000). The lin-41 RBCC gene acts in the *C. elegans* heterochronic pathway between the let-7 regulatory RNA and the LIN-29 transcription factor. Mol. Cell *5*, 659–669.

Stocker, H., and Hafen, E. (2000). Genetic control of cell size. Curr. Opin. Genet. Dev. *10*, 529–535.

Teleman, A.A., Strigini, M., and Cohen, S.M. (2001). Shaping morphogen gradients. Cell *105*, 559–562.

Thompson, B., Townsley, F., Rosin-Arbesfeld, R., Musisi, H., and Bienz, M. (2002). A new nuclear component of the Wnt signalling pathway. Nat. Cell Biol. *4*, 367–373.

Wightman, B., Ha, I., and Ruvkun, G. (1993). Posttranscriptional regulation of the heterochronic gene lin-14 by lin-4 mediates temporal pattern formation in *C. elegans*. Cell *75*, 855–862.

Yoo, S.J., Huh, J.R., Muro, I., Yu, H., Wang, L., Wang, S.L., Feldman, R.M., Clem, R.J., Muller, H.A., and Hay, B.A. (2002). Hid, Rpr and Grim negatively regulate DIAP1 levels through distinct mechanisms. Nat. Cell Biol. *4*, 416–424.

Yu, S.Y., Yoo, S.J., Yang, L., Zapata, C., Srinivasan, A., Hay, B.A., and Baker, N.E. (2002). A pathway of signals regulating effector and initiator caspases in the developing *Drosophila* eye. Development *129*, 3269–3278.

Zeng, W., Wharton, K.A., Jr., Mack, J.A., Wang, K., Gadbaw, M., Suyama, K., Klein, P.S., and Scott, M.P. (2000). Naked cuticle encodes an inducible antagonist of Wnt signalling. Nature *403*, 789–795.

Zeng, Y., Wagner, E.J., and Cullen, B.R. (2002). Both natural and designed micro RNAs can inhibit the expression of cognate mRNAs when expressed in human cells. Mol. Cell *9*, 1327–1333.

Zhang, J., and Carthew, R.W. (1998). Interactions between wingless and DFz2 during *Drosophila* wing development. Development *125*, 3075–3085.

Accession Numbers

The GenBank accession number for the *bantam* miRNA sequence reported in this paper is AJ550546.

Note Added in Proof

Léopold and colleagues have independently identified *bantam* as a gene involved in growth regulation (Raisin, S., Pantalacci, S., Breittmeyer, J.-P. and Léopold, P. (2003). A new genetic locus controlling growth and proliferation in *Drosophila melanogaster*. Genetics, in press).